Supplemental Materials

Molecular Biology of the Cell

Yuan et al.

Online supplemental material

Qualitative minimal model for the G1/S transition

Based on our experimental observations, we have proposed a minimal model for cyclinE-CDK2 activation during the G1/S transition. Our model shows a bistable behavior at steady state, as well as the switching of active CDK2 from lower to a higher level in the temporal regime, suggestive of S-phase onset.

According to our model (Figure 9A) cyclin E and CDK2 associate to form cyclinE-CDK2-P (Active CDK2). p27, which is synthesized at a constant rate, combines with Active CDK2 to form an inhibitory complex: cyclinE-CDK2-P-p27. Active CDK2 then phosphorylates this complex upon a residue within p27 to yield another complex cyclinE-CDK2-P-p27-P. This complex is targeted by SCF^{Skp2}, and results in the ubiquitylation of p27 and the subsequent release of Active CDK2. This forms a positive-feedback loop where Active CDK2 activates itself by trans-phosphorylating p27. In addition to this, p27 is also degraded by Skp2, independent of CDK2 (Bloom and Pagano, 2003; Chu *et al.*, 2008). In our model,"Skp2" is a parameter rather than a variable, for simplicity. The reactions and rate equations are given in the Table S1, and corresponding parameters are given in the Table S2. We simulated the model using Systems Biology Workbench (SBW) (Bergmann and Sauro, 2006), and the steady state bifurcation diagrams were generated using XPPAUT,which is available at http://www.math.pitt.edu/~bard/xpp/xpp.html (Ermentrout and Mahajan, 2003).

When simulated, our model shows temporal switching of Active CDK2 from a low to a high level indicating the G1/S transition (Figure 9C – black). In Cdh1 ablated cells, accumulation of Skp2 results in the early activation of SCF^{Skp2}. We have represented this in the model by progressively increasing the level of Skp2. For simplicity, we assume the same parameter "Skp2" affects the p27 as well as cyclinE-CDK2-P-p27-P degradation. In Cdh1-depleted cells, the G1/S transition occurs at a much earlier time, indicating premature activation of CDK2 and early S phase onset (Figure 9C - red, blue, and green). Consistent with our experimental data, our model also shows that the amount of total cyclin E abundance in Cdh1-ablated G1 cells is less than that of control. In addition to this, the steady-state parameter diagram (Figure 9D) also shows a weakening of the positive feedback loop where the width of the hysteresis curve decreases as Skp2 levels increase. We have not included E2F-mediated cyclin E synthesis and a proteolysis pathway for cyclin E depletion for simplicity, and hence, we observe constant levels of total cyclin E abundance post-G1/S transition, as well as the absence of an oscillatory cell cycle. Nevertheless, this simple model captures the important aspects of the positive-feedback generated in part by APC-Cdh1, and its weakening effect when Cdh1 levels are decreased.

We also explored the behavior of the model representing p27 knockdown. p27 knockdown can be represented by reducing the synthesis rate of p27 namely k_{syn_p27}. The phenotype is similar to that of Cdh1 knockdown (Figures 9E-G).

Important features of the model:

- The model exhibits bistability in Active CDK2 levels in response to total CDK2 levels. We observed bistability for the ratio of $k_{syn\_cycE} / k_{deg\_cycE} \geqslant 0.6$ and $k_{ass\_p27} / k_{diss\_p27} \geqslant 0.8$. As $k_{syn\_cycE} / k_{deg\_cycE}$ (and $k_{ass\_p27} / k_{diss\_p27}$) increases, bistability becomes more and more prominent.
- In our model, the total [cycE abundance] was 1.2 folds less than that of overall [Total CDK2] levels (Figures 9B-G). However experiments , it has have shown that the total [cycE abundance] was about 8-fold less than [Total CDK2] in HeLa cells (Arooz *et al.*, 2000). The discrepancy in the model could be due to the fact that it does not include mechanisms such as cycE degradation.

- It is important to note that this model is only an exploratory tool based on our hypothesis and the observations in the model are only suggestive of what might be happening in the system. All parameters in the model are arbitrary since experimental values for most chemical reactions are unavailable.

Table S1: Reactions and rate equations representing the model shown in Figure 9A

Reactions	Rates
Source $\rightarrow$ cycE	R_1: k_{syn_cycE}
cycE $\rightarrow$ Sink	R_2: k_{deg_cycE} [cycE]
cycE + CDK2 $\rightleftarrows$ cycE-CDK2-P	R_3: k_{ass_cycE} [cycE][CDK2] – k_{diss_cycE} [cycE-CDK2-P]
Source $\rightarrow$ p27	R_4: k_{syn_p27}
p27 $\xrightarrow{Skp2}$ Sink	R_5: k_{deg_p27} [Skp2][p27]
p27 + cycE-CDK2-P $\rightleftarrows$ cycE-CDK2-P-p27	R_6: k_{ass_p27}[p27][cycE-CDK2-P] $-k_{diss\_p27}$[cycE-CDK2-P-p27]
cycE-CDK2-P-p27 $\rightarrow$ cycE-CDK2-P-p27-P	R_7: k_{phos_p27}[cycE-CDK2-P] [cycE-CDK2-P-p27]
cycE-CDK2-P-p27-P $\xrightarrow{Skp2}$ cycE-CDK2-P + p27-P	R_8: k_{skp2}[Skp2] [cycE-CDK2-P-p27-P]

Ordinary Differential Equations:

$$d[cycE]/dt = R_1 - R_2 - R_3$$
$$d[CDK2]/dt = -R_3$$
$$d[cycE\text{-}CDK2\text{-}P]/dt = R_3 - R_6 + R_8$$
$$d[cycE\text{-}CDK2\text{-}P\text{-}p27]/dt = R_6 - R_7$$
$$d[cycE\text{-}CDK2\text{-}P\text{-}p27\text{-}P]/dt = -R_6 + R_7 - R_8$$
$$d[p27]/dt = R_4 - R_5 - R_6$$

All species initial concentration = 0 except $[CDK2]_{t=0}$ =30.

[cycE abundance] = [cycE] + [cycE-CDK2-P] + [cycE-CDK2-P-p27] + [cycE-CDK2-P-p27-P]
[Total p27] = [p27] + [cycE-CDK2-P-p27] + [cycE-CDK2-P-p27-P]
[Total CDK2] = [CDK2] + [cycE-CDK2-P] + [cycE-CDK2-P-p27] + [cycE-CDK2-P-p27-P]=30

Table S2: Parameters used in the model

Parameters	Description	Units	Value used in simulation
k_{syn_cycE}	Synthesis rate of cyclin E	Conc. $Time^{-1}$	0.18
k_{deg_cycE}	Degradation rate of cyclin E	$Time^{-1}$	0.3
k_{ass_cycE}	Association constant of CDK2 with cyclin E	$Conc^{-1}Time^{-1}$	0.01
k_{diss_cycE}	Dissociation constant of CDK2-cyclin E complex	$Time^{-1}$	0.001
k_{syn_p27}	Synthesis rate of p27	$Conc.Time^{-1}$	1
k_{deg_p27}	Degradation rate of p27	$Time^{-1}$	0.5
[Skp2]	Concentration of Skp2	Conc.	1,1.5, and 3 (varies)
k_{ass_p27}	Association constant of active CDK2 with p27	$Conc^{-1}Time^{-1}$	8
k_{diss_p27}	Dissociation constant of CDK2-p27 complex	$Time^{-1}$	0.4
k_{phos_p27}	Phosphorylation constant of cycE-CDK2-P-p27	$Conc^{-1}Time^{-1}$	0.02
k_{skp2}	Rate constant for SCF^{Skp2} interaction	$Conc^{-1}Time^{-1}$	0.5

Additional statistical information for primary figures

Figure 1. Depletion of Cdh1 shortened G1-phase duration in HeLa cells. (B) GL2-siRNA: mean, 525.86 min; 95% CI, 515.04-536.66 min. Cdh1-siRNA: mean, 321.63 min; 95% CI, 312.09-331.18 min. Cdc20-siRNA: mean, 500.10 min; 95% CI, 484.34-515.86 min. ANOVA and *post-hoc* Dunnett's T3 test were used to determine the statistical difference between the timing of each siRNA treatment, and significance values were indicated (**, $P < 0.001$; *, $P < 0.05$).

Figure 2. Cdh1 knockdown in HeLa cells altered the kinetics of cyclin B1 and E1 accumulation and caused early transcription of certain E2F1 targets. (D) The paired Student's t-Test was used to determine the statistical difference between GL2-siRNA transfected samples and Cdh1-siRNA transfected samples.

Figure 3. Precocious cyclin E1 accumulation corresponds with early S-phase onset in Cdh1 depleted cells. (B) GL2-siRNA: mean, 564.28 min; 95% CI, 540.77-587.79 min. Cdh1-siRNA: mean, 376.41 min; 95% CI, 361.11-391.72 min. Cdh1/CycA2-siRNA: mean, 350.06 min; 95% CI, 332.50-367.61 min. Cdh1/CycB1-siRNA: mean, 412.86 min; 95% CI, 396.29-429.44 min. Cdh1/CycE1-siRNA: mean, 476.36 min; 95% CI, 454.77-497.96 min. ANOVA and *post-hoc* Dunnett's T3 test were used to determine the statistical difference between the timing of each siRNA treatment, and significance values were indicated (**, $P < 0.001$; *, $P < 0.05$).

Figure 4. Overexpressing p27 recovered G1-phase duration in Cdh1-depleted cells. (E) GL2-siRNA: mean, 581.83 min; 95% CI, 568.99-594.68 min. Cdh1-siRNA: mean, 400.04 min; 95% CI, 388.80-411.29 min. Cdh1-siRNA/pECFP-p27: mean, 459.53; 95% CI, 444.81-474.24 min. ANOVA and *post-hoc* Dunnett's T3 test were used to determine the statistical difference between the timing of each siRNA treatment, and significance values were indicated.

Figure 5. Cdh1 depletion altered the pattern of cyclin E accumulation in cells progressing from G1 to S phase. (C) For each of three replicate experiments, 30,000 G1-phase-gated cells were randomly sampled from each treatment, and data were multiplied by a factor to center and scale the results. Normalized data were then pooled and square-rooted to obtain normality, and probability densities for each treatment were then plotted ($p < 0.001$) (D) Total cyclin E1 contents of 154,751 GL2 siRNA-transfected cells and 282,860 Cdh1-siRNA transfected cells from three experiments were analyzed, and data were then subdivided and pooled into 10 equivalent bins of increasing DNA content. Welch's t-test was used to determine the statistical difference between treatments within each respective bin. For all bins, $p < 0.001$.

Figure 6. Partial knockdown of p27 mirrors the acceleration of S-phase onset caused by Cdh1 loss. (C) For each of two replicate experiments, 19,000 G1-phase-gated cells were randomly sampled from each treatment, and data were multiplied by a factor to center and scale the results. Normalized data were then pooled and square-rooted to obtain normality, and probability densities for each treatment were then plotted ($p < 0.001$ for all comparisons). (D) Total cyclin E1 contents of 77,795 GL2 siRNA-transfected cells, 116,043 Cdh1 siRNA transfected cells, and 116,021 p27 siRNA-transfected cells from two experiments were analyzed, and data were then subdivided and pooled into 10 equivalent bins of increasing DNA content. Welch's t-test was used to determine the statistical difference between treatments within each respective bin. For Cdh1 versus GL2, $p < 0.001$ for all bins. For Cdh1 versus p27,

$p < 0.001$ for all bins. For GL2 versus p27, $p < 0.001$ for bins S1-S4, $p < 0.05$ for bins S5 and S10, and $p > 0.05$ for bins S6-S9.

Figure 7. Cdh1 ablation accelerates S-phase onset and prolongs its duration. (B) GL2-siRNA: mean, 595.85 min; 95% CI, 579.87-611.83 min. Cdh1-siRNA: mean, 436.09 min; 95% CI, 420.11-452.07 min. GL2-siRNA/pECFP-CycE1: mean, 442.19 min; 95% CI, 426.21-458.17 min; Cdh1-siRNA/pECFP-CycE1: mean, 404.40 min; 95% CI, 388.42-420.38 min. ANOVA and *post-hoc* Dunnett's T3 test were used to determine the statistical difference between the timing of each siRNA treatment, and significance values were indicated (**, $P < 0.001$; *, $P < 0.05$). (C) GL2-siRNA: mean, 63.30; 95% CI, 61.48-65.11. Cdh1-siRNA: mean, 45.13; 95% CI, 43.23-47.03. GL2-siRNA/pECFP-CycE1: mean, 61.12; 95% CI, 58.79-63.45; Cdh1-siRNA/pECFP-CycE1: mean, 44.27; 95% CI, 41.75-46.78. ANOVA and *post-hoc* Dunnett's T3 test were used to determine the statistical difference between the timing of each siRNA treatment, and significance values are indicated (**, $P < 0.001$). (D) GL2-siRNA: mean, 656.84 min; 95% CI, 636.86-676.82 min. Cdh1-siRNA: mean, 792.96 min; 95% CI, 774.88-811.05 min. GL2-siRNA/pECFP-CycE1: mean, 710.49 min; 95% CI, 691.36-729.62 min; Cdh1-siRNA/pECFP-CycE1: mean, 807.77 min; 95% CI, 787.11-828.43 min. ANOVA and *post-hoc* Dunnett's T3 test were used to determine the statistical difference between the timing of each siRNA treatment, and significance values were indicated (**, $P < 0.001$; *, $P < 0.05$)

Figure 8. Cdh1 loss slowed the rate of replication fork elongation and decreased the frequency of termination events. (C) Average fork elongation rate was calculated using the following formula: (number of pixels of green tracks in red-green-tracks/2.2)*3862 nucleotides/20 minutes. ANOVA was used to determine the statistical difference between the rates of each siRNA treatment, and significance was indicated. GL2-siRNA: mean, 2376.45; SEM, 92.51. Cdh1-siRNA: mean, 1897.21; SEM, 101.29. (D) Welch's t-test was used to determine the statistical difference between the number of forks per Mb of each siRNA treatment, and significance is indicated. GL2-siRNA: mean, 21.26; SEM, 0.57. Cdh1-siRNA: mean, 24.30; SEM, 0.74. (E) Pearson's Chi-squared test was used to determine the statistical difference between the frequencies in Cdh1-depleted and control cells, and significance is indicated ($p>0.05$; difference is insignificant). (F) Pearson's Chi-squared test was used to determine the statistical difference the frequencies in between Cdh1-depleted and control cells, and significance was indicated.

Supplementary figure legends

Figure S1. Depletion of Cdh1 decreased the G1-phase population and increased the S-phase population. (A) Immunoblots for indicated proteins in HeLa cell lysates (30 μg total protein) after siRNA transfection with or without a Cdh1-rescue plasmid. Two asterisks indicate endogenous Cdh1; one indicates ectopic pECFP-mutCdh1. (B) Cell cycle distributions of cells in (A), determined by EdU labeling and propidium iodide (PI) staining, followed by flow cytometry. Data were plotted as means±SEM (N=2). (C) Pseudo-color scatter plots of representative experiment shown in Figure 1E plotting DNA content vs. EdU content in 50,000 cells after transfections with siRNAs directed towards GL2 or Cdh1 with or without a Cdh1-rescue plasmid.

Figure S2. Histograms of DNA content of GL2- and Cdh1-siRNA transfected cells following triple thymidine block and release. Cell samples were collected at the indicated time points following release from a triple-thymidine block, fixed and stained for DNA content, and then analyzed by flow cytometry.

Figure S3. Cyclin E1 and not B1 stimulated early S-phase entry in Cdh1-depleted cells. (A) Immunoblots for Cdh1, cyclin B1, cyclin E1, Skp2, and tubulin in HeLa cell lysates (30 μg of protein) after indicated siRNA transfection for live cell imaging. (B) Plot of average G1 duration times for GL2-, Cdh1-, Cdh1/cyclin E1, and Cdh1/cyclin B1/cyclin E1-siRNA transfected cells. Transfections and imaging were performed in triplicate (N=3; n_{GL2}=242, n_{Cdh1}=323, $n_{Cdh1/CycE1}$=259, $n_{Cdh1/CycB1/CycE1}$=202 representative cells). Errors bars represent the distribution of average G1 duration in each group with a confidence interval of 95% (95% CI). GL2-siRNA: mean, 578.09 min; 95% CI, 563.99-592.19 min. Cdh1-siRNA: mean, 411.82 min; 95% CI, 399.62-424.03 min. Cdh1/CycE1-siRNA: mean, 524.62 min; 95% CI, 511.00-538.25 min. Cdh1/CycB1/CycE1-siRNA: mean, 497.28 min; 95% CI, 481.85-512.71 min. ANOVA and *post-hoc* Dunnett's T3 test were used to determine the statistical difference between the timing of each siRNA treatment, and significance were indicated (**, $P < 0.001$; *, $P < 0.05$).

Figure S4. Knockdown of cyclin E1 prolongs G1 phase in cells with or without Cdh1. (A) Immunoblots probing for Cdh1, cyclins (A2, B1, and E1), and tubulin in HeLa cell lysates (30 μg total protein) after indicated siRNA transfection for flow cytometry. (B) Immunoblots probing for Cdh1, cyclin E1, and tubulin in HeLa cell lysates (30 μg total protein) after indicated siRNA transfections. (C) Cell cycle distributions of cells in (B), determined by EdU labeling and propidium iodide (PI) staining, followed by flow cytometry.

Figure S5. Expression of p27 prolongs G1 phase in cells with or without Cdh1. (A) Immunoblots probing for Cdh1, cyclins (A2, B1, and E1), and tubulin in HeLa cell lysates (30μg of total protein) after indicated siRNA transfection for flow cytometry. (B) Immunoblots probing for Cdh1, cyclin E1, p27, Skp2, and tubulin in HeLa cell lysates (30 μg of total protein) after siRNA transfection with or without a pECFP-p27 for flow cytometry. Two asterisks indicates endogenous p27, one asterisk indicates ectopic pECFP-p27. (C) Cell cycle distribution of cells in (B) was determined by EdU labeling, PI staining, and flow cytometry. Data were plotted as means±SEM (N=3).

Figure S6. Cyclin A protein content remains unchanged whereas cyclin B protein content is increased during G1 and S phases in Cdh1-depleted cells. HeLa cells were transfected with siRNAs directed against GL2 or Cdh1 during a triple-thymidine block, and following their release, were

collected and fixed at the indicated time points, and then probed for their DNA content and either cyclin A2 (A) or cyclin B1 abundance (B). Cells were then analyzed by flow cytometry.

Figure S7. APC-Cdh1 function is required to permit proper accumulation of p27 and cyclin E1 in HeLa cells. (A) Asynchronous HeLa cells that were unstained with primary antibody but stained with anti-rabbit (488 nm conjugate; "p27 abundance") and anti-mouse (647 nm conjugate; "cyclin E1 abundance") secondary antibodies. Gates were then drawn to include a majority of cells (≈98%) in the "p27-/cyclin E1-" quadrant, and these were then used to generate the DNA histograms shown in Figure 6. (B) Bivariate zebra plots of siRNA-transfected HeLa cells that were thymidine blocked, released, and collected over the indicated time points. The zoomed inset highlights both the zebra and pseudocolor plots that indicate three distinct p27/cyclin E subpopulations present at 22 h (p27+/cycE-; p27+/cycE+; p27-/cycE+).

Figure S8. DNA damage responses were undetectable in Cdh1-depleted HeLa cells. (A) Pseudo-color scatter plots of DNA content vs. p-Chk1 (S345), p-Chk2 (T68), or p-H2AX (S139) in 30,000 cells treated with DMSO or titrated with increasing amounts of hydroxyurea (HU) or aphidicolin. (B) Immunoblots probing for Cdh1, p27, pS345-Chk1, Skp2, and tubulin in HeLa cell lysates (30 µg of total protein) after indicated siRNA transfection for 2 or 5 days, compared to HU- or aphidicolin-treated controls. (C) Pseudo-color scatter plots of DNA content vs. p-Chk1 (S345), p-Chk2 (T68), or p-H2AX (S139) in 30,000 cells described in (B).

Figure S9. DNA damage responses were undetectable in Cdh1-depleted HeLa and U2OS cells. (A) Immunoblots probing for Cdh1, p27, pS345-Chk1, and tubulin in HeLa cell lysates (35 µg protein) after indicated siRNA transfections, compared to 2 mM HU-treated control. (B) Pseudo-color scatter plots of DNA content vs. p-Chk1 (S345), p-Chk2 (T68), or p-H2AX (S139) in 10000 cells described in (A). (C) Immunoblots probing for Cdh1, p27, pS345-Chk1, and tubulin in U2OS cell lysates after indicated siRNA transfection compared to 2 mM HU treated control. (D) Pseudo-color scatter plots of DNA content vs. p-Chk1 (S345), p-Chk2 (T68), or p-H2AX (S139) in 10000 cells described in (C)

Figure S10. No increase of pS139-H2AX signal was detectable in either HeLa or U2OS cells after Cdh1 or p27 depletion. (A) Representative images of immunofluorescence staining for pS139-H2AX (green) and DAPI (blue) under 20×-objective in HeLa and U2OS cells transfected with indicated siRNAs compared to a 2 mM HU-treated control. (B) Histogram of frequencies of pS139-H2AX positive HeLa cells after GL2-, Cdh1-, or p27-siRNA transfection or HU treatment (N=2, n_{HU}= 3023, n_{GL2}=2794, n_{Cdh1}=2880, n_{p27}=2834). (C) Histogram of frequencies of pS139-H2AX-positive U2OS cells after GL2-, Cdh1-, or p27-siRNA transfection or HU treatment (N=2, n_{HU}= 2369, n_{GL2}=2314, n_{Cdh1}=2653, n_{p27}=2303). Chi-square test was used to determine the statistical difference of each treatment compared with GL2-transfected control, and significance was indicated (**, $P < 0.001$).

Figure S11. Cdh1 depletion increases a CDK2-specific phosphorylation of Rb (pT821) in HeLa cells. (A) Immunoblots for indicated proteins in HeLa cell lysates (35 µg protein) prepared at indicated time points after GL2- and Cdh1-siRNA transfection with triple thymidine block and release.
(B) Quantitation of pT821-Rb signals were done using ImageJ, and values were normalized to anti-tubulin signal and plotted as means±SD (N=2).

References

Arooz, T., Yam, C.H., Siu, W.Y., Lau, A., Li, K.K.W., and Poon, R.Y.C. (2000). On the Concentrations of Cyclins and Cyclin-Dependent Kinases in Extracts of Cultured Human Cells,Ä†. Biochemistry *39*, 9494-9501.

Bergmann, F.T., and Sauro, H.M. (2006). SBW-a modular framework for systems biology. Proceedings of the 38th conference on Winter simulation, 1637-1645.

Bloom, J., and Pagano, M. (2003). Deregulated degradation of the cdk inhibitor p27 and malignant transformation. Seminars in Cancer Biology *13*, 41-47.

Chu, I.M., Hengst, L., and Slingerland, J.M. (2008). The Cdk inhibitor p27 in human cancer: prognostic potential and relevance to anticancer therapy. Nat Rev Cancer *8*, 253-267.

Ermentrout, B., and Mahajan, A. (2003). Simulating, analyzing, and animating dynamical systems: a guide to XPPAUT for researchers and students. Applied Mechanics Reviews *56*, 53.

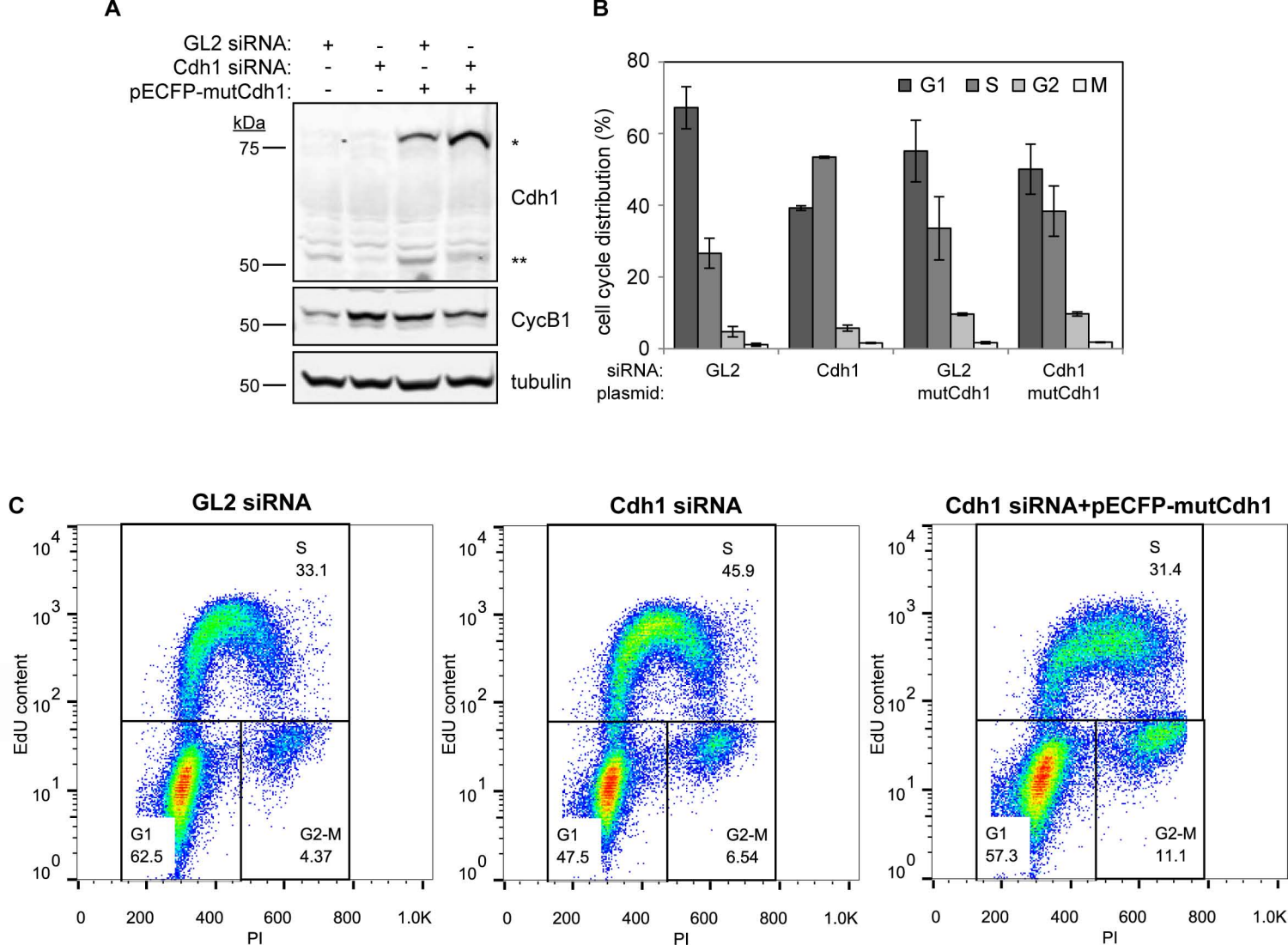
A
GL2 siRNA: + - + -
Cdh1 siRNA: - + - +
pECFP-mutCdh1: - - + +
kDa
75
50
50
50
*
Cdh1
**
CycB1
tubulin
B
cell cycle distribution (%)
80
60
40
20
0
G1
S
G2
M
siRNA: GL2 Cdh1 GL2 Cdh1
plasmid: mutCdh1 mutCdh1
C
GL2 siRNA
Cdh1 siRNA
Cdh1 siRNA+pECFP-mutCdh1
EdU content
PI
S
33.1
G1
62.5
G2-M
4.37
S
45.9
G1
47.5
G2-M
6.54
S
31.4
G1
57.3
G2-M
11.1
0
200
400
600
800
1.0K

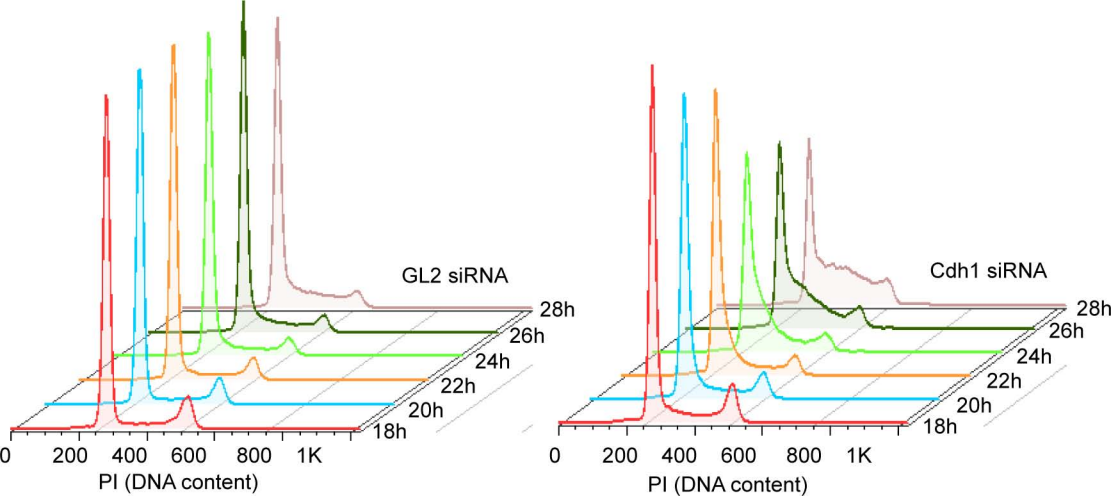
GL2 siRNA
28h
26h
24h
22h
20h
18h
0
200
400
600
800
1K
PI (DNA content)
Cdh1 siRNA
28h
26h
24h
22h
20h
18h
0
200
400
600
800
1K
PI (DNA content)

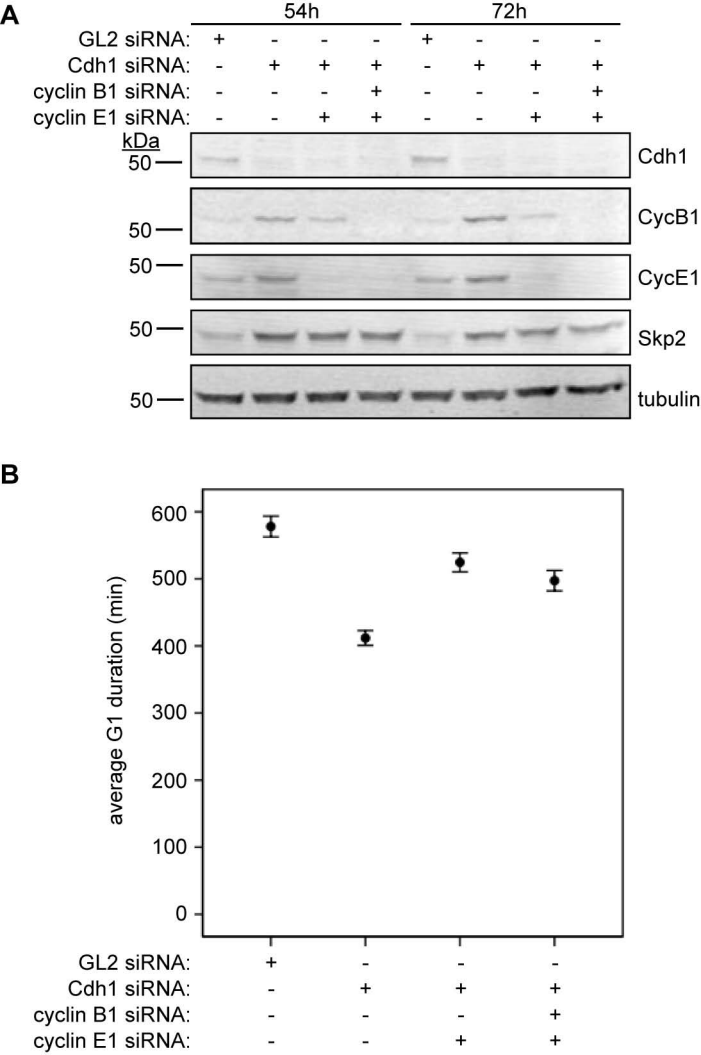
A
54h
72h
GL2 siRNA: + - - - + - - -
Cdh1 siRNA: - + + + - + + +
cyclin B1 siRNA: - - - + - - - +
cyclin E1 siRNA: - - + + - - + +
kDa
50
Cdh1
CycB1
CycE1
Skp2
tubulin
B
average G1 duration (min)
600
500
400
300
200
100
0
GL2 siRNA: + - - -
Cdh1 siRNA: - + + +
cyclin B1 siRNA: - - - +
cyclin E1 siRNA: - - + +

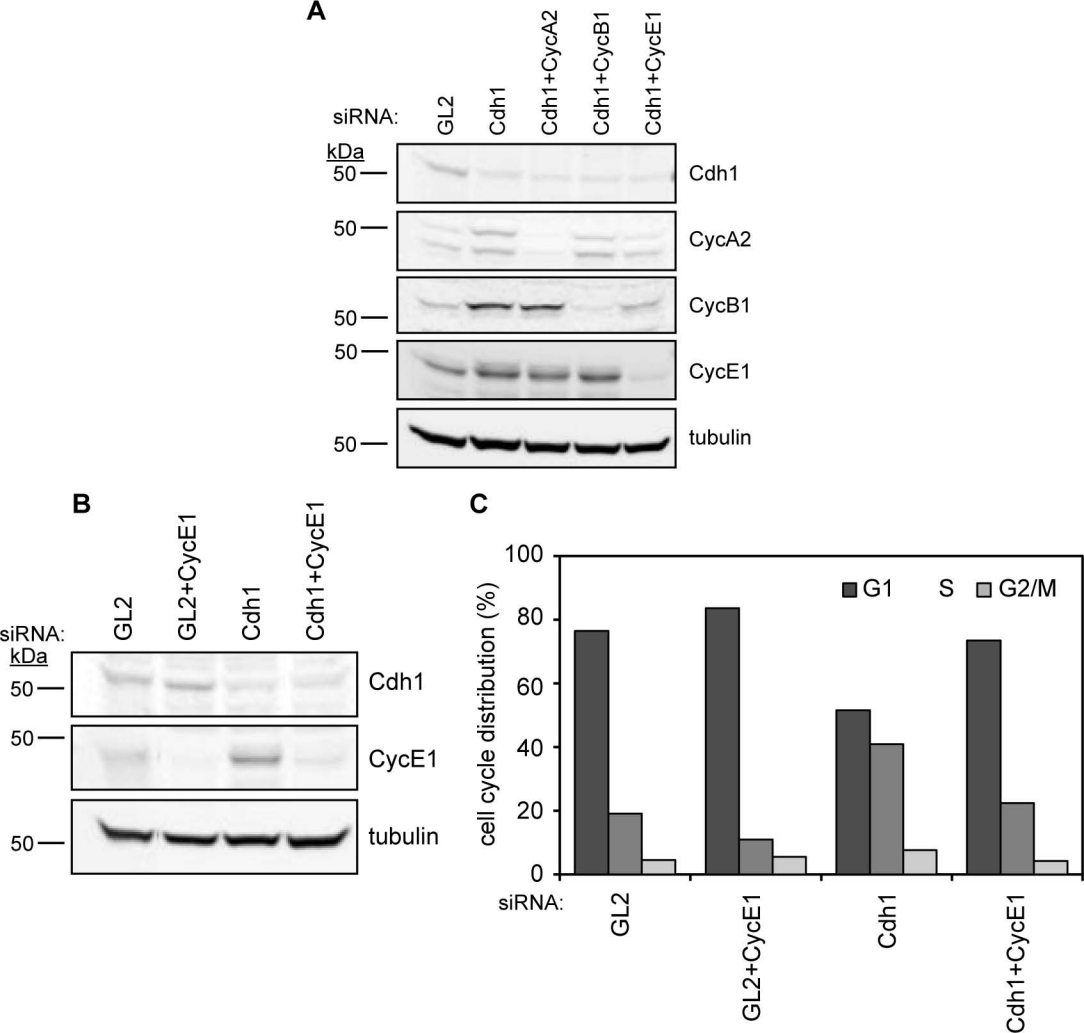
A
siRNA:
GL2
Cdh1
Cdh1+CycA2
Cdh1+CycB1
Cdh1+CycE1
kDa
50
Cdh1
CycA2
CycB1
CycE1
tubulin
B
GL2
GL2+CycE1
Cdh1
Cdh1+CycE1
C
cell cycle distribution (%)
100
80
60
40
20
0
G1
S
G2/M

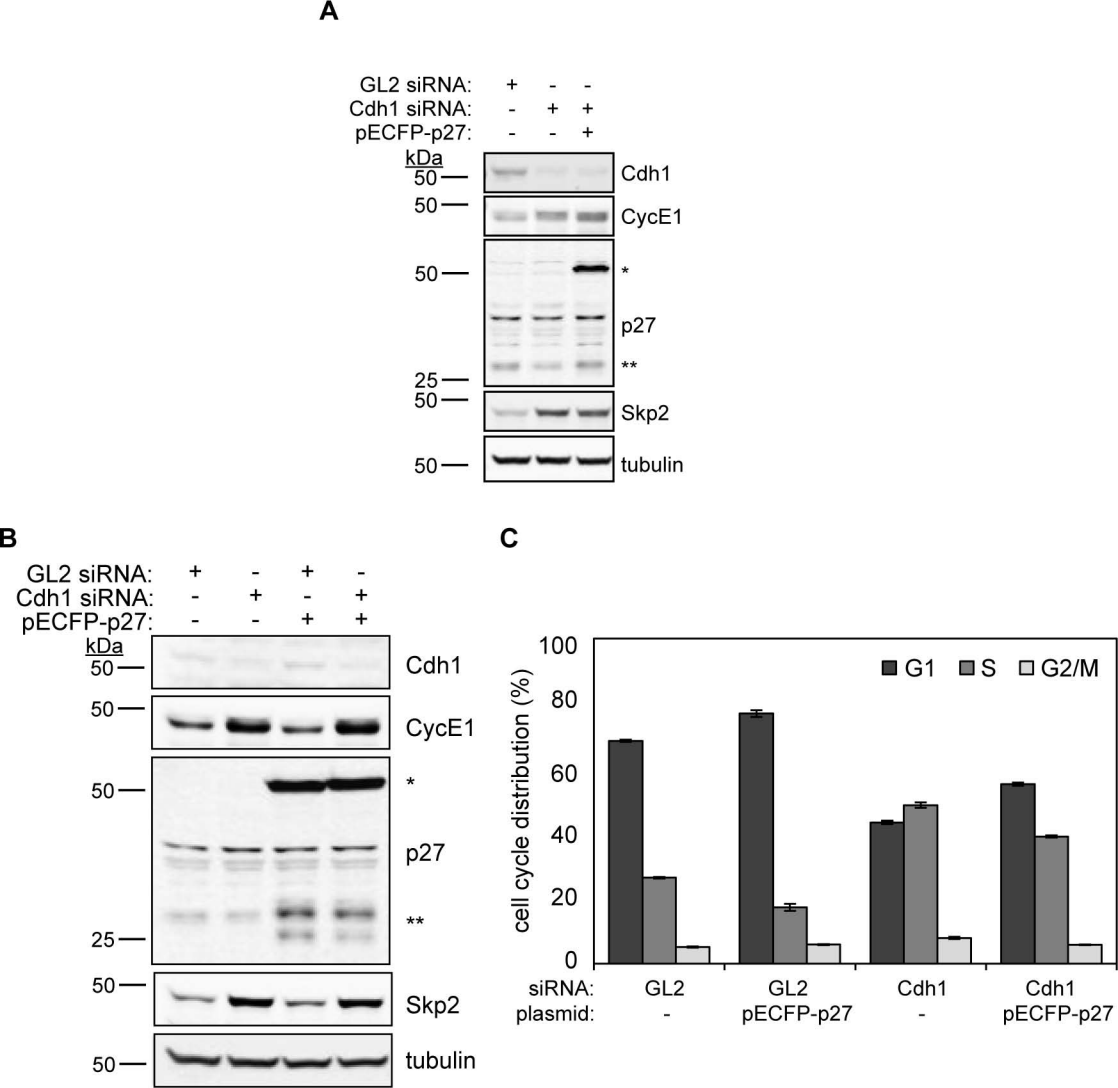
A
GL2 siRNA: + - -
Cdh1 siRNA: - + +
pECFP-p27: - - +
kDa
50
Cdh1
50
CycE1
50
*
p27
**
25
50
Skp2
50
tubulin
B
GL2 siRNA: + - + -
Cdh1 siRNA: - + - +
pECFP-p27: - - + +
kDa
50
Cdh1
50
CycE1
50
*
p27
**
25
50
Skp2
50
tubulin
C
cell cycle distribution (%)
100
80
60
40
20
0
G1
S
G2/M
siRNA: GL2 GL2 Cdh1 Cdh1
plasmid: - pECFP-p27 - pECFP-p27

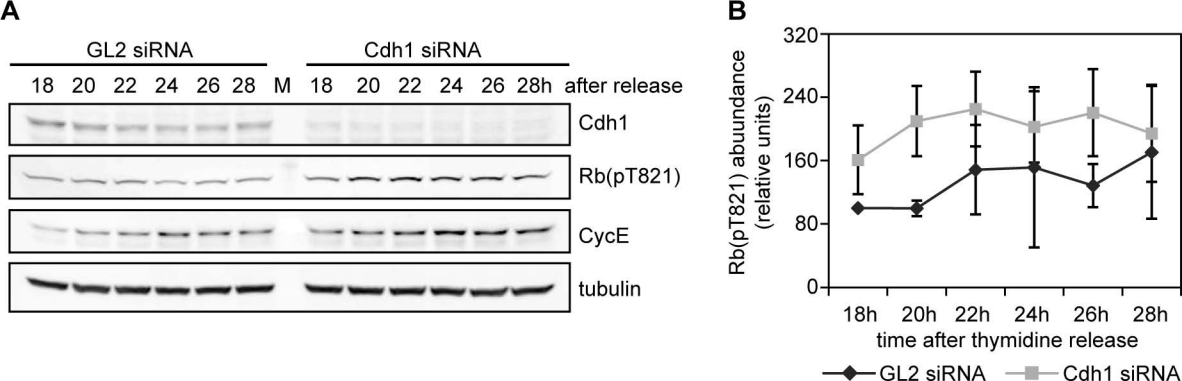
A
GL2 siRNA
Cdh1 siRNA
18 20 22 24 26 28 M 18 20 22 24 26 28h after release
Cdh1
Rb(pT821)
CycE
tubulin
B
Rb(pT821) abuundance (relative units)
320
240
160
80
0
18h 20h 22h 24h 26h 28h
time after thymidine release
GL2 siRNA
Cdh1 siRNA

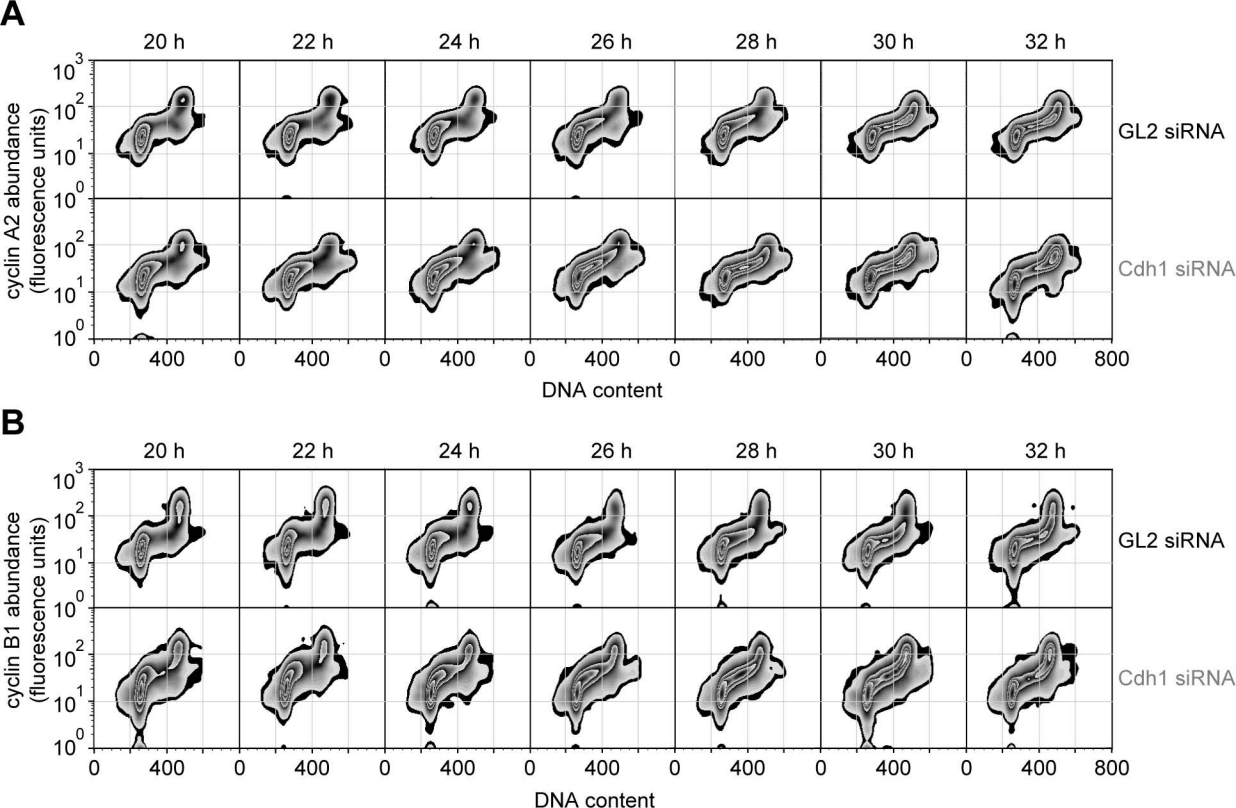
A
20 h
22 h
24 h
26 h
28 h
30 h
32 h
cyclin A2 abundance (fluorescence units)
GL2 siRNA
Cdh1 siRNA
DNA content
B
20 h
22 h
24 h
26 h
28 h
30 h
32 h
cyclin B1 abundance (fluorescence units)
GL2 siRNA
Cdh1 siRNA
DNA content

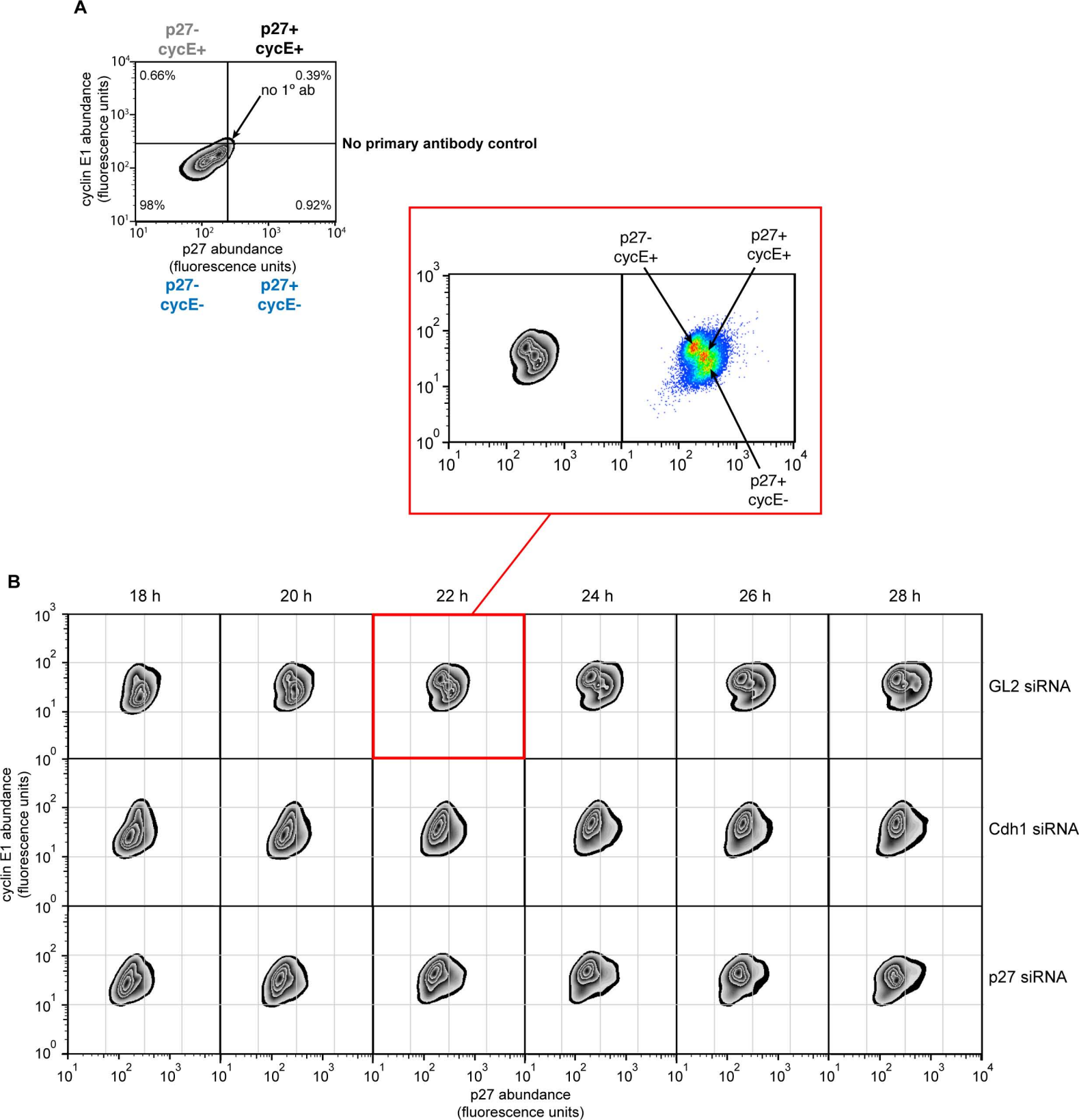
A
p27-
cycE+
p27+
cycE+
0.66%
0.39%
no 1° ab
98%
0.92%
cyclin E1 abundance
(fluorescence units)
p27 abundance
(fluorescence units)
p27-
cycE-
p27+
cycE-
No primary antibody control
p27-
cycE+
p27+
cycE+
p27+
cycE-
B
18 h
20 h
22 h
24 h
26 h
28 h
GL2 siRNA
Cdh1 siRNA
p27 siRNA
cyclin E1 abundance
(fluorescence units)
p27 abundance
(fluorescence units)

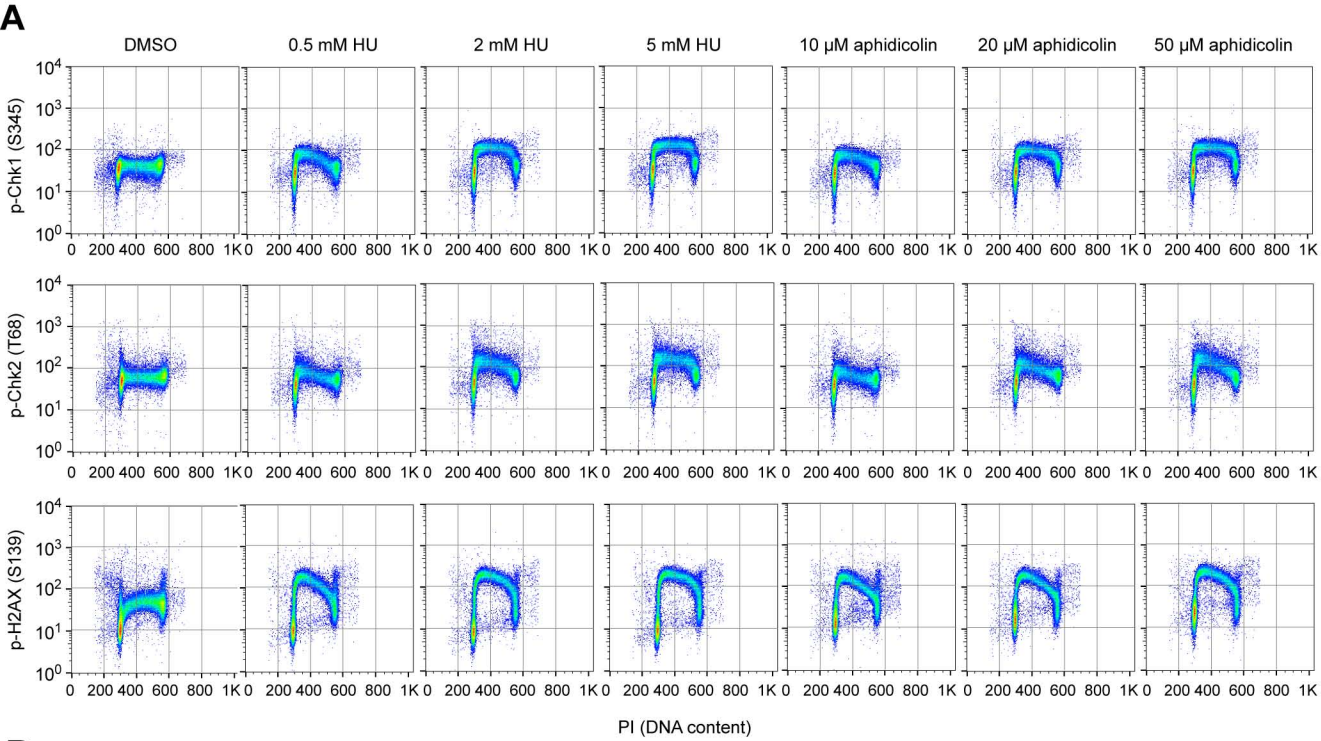
A
DMSO
0.5 mM HU
2 mM HU
5 mM HU
10 μM aphidicolin
20 μM aphidicolin
50 μM aphidicolin
p-Chk1 (S345)
p-Chk2 (T68)
p-H2AX (S139)
PI (DNA content)

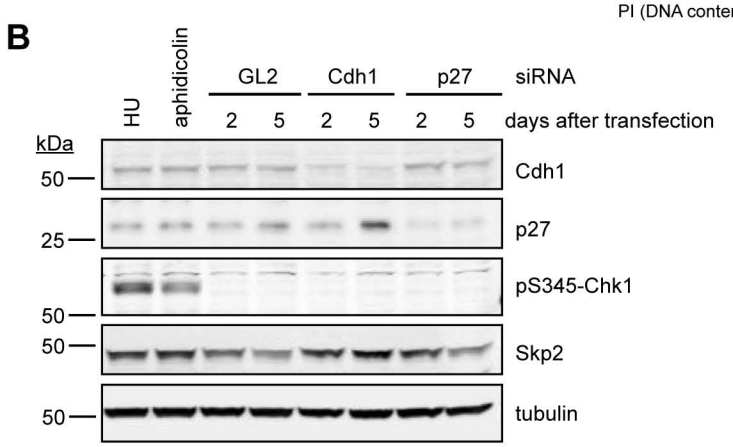
B
HU
aphidicolin
GL2
Cdh1
p27
siRNA
2
5
2
5
2
5
days after transfection
kDa
50
25
50
50
50
Cdh1
p27
pS345-Chk1
Skp2
tubulin

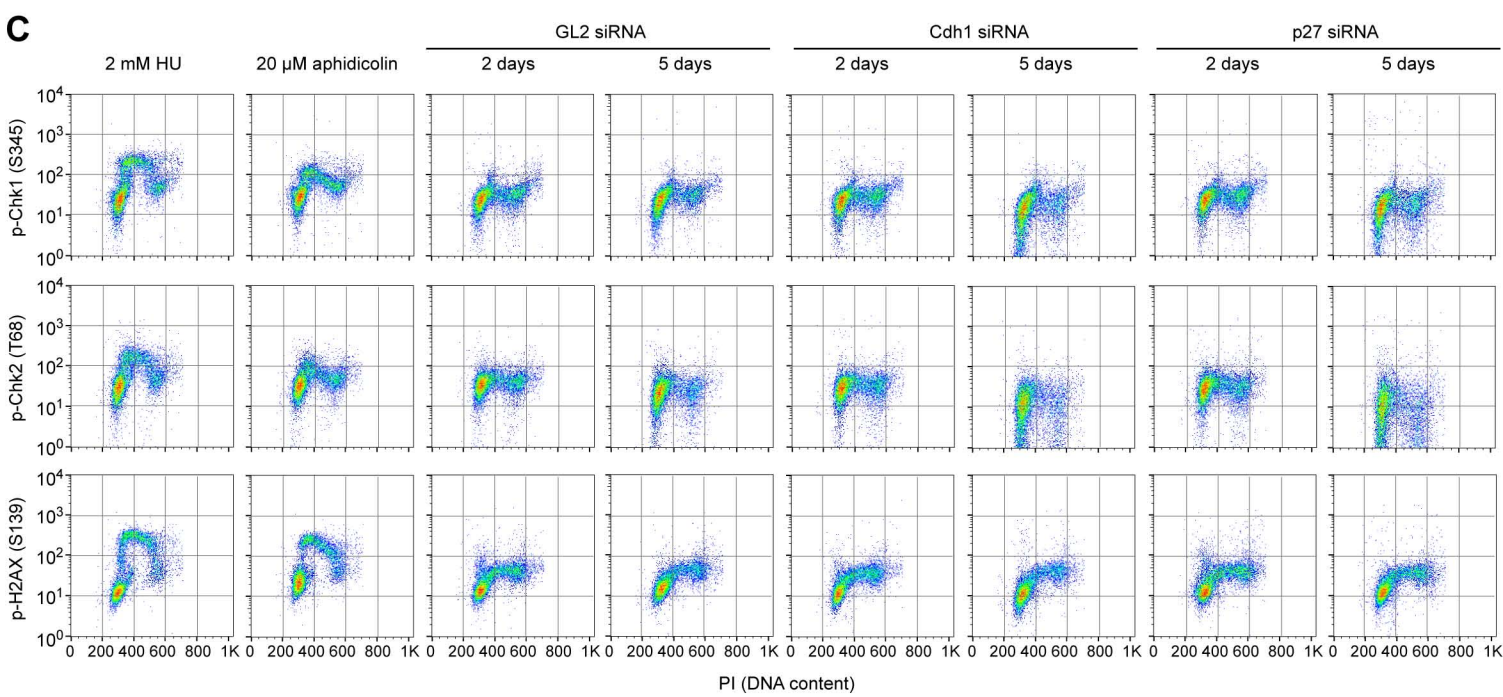
C
2 mM HU
20 μM aphidicolin
GL2 siRNA
Cdh1 siRNA
p27 siRNA
2 days
5 days
2 days
5 days
2 days
5 days
p-Chk1 (S345)
p-Chk2 (T68)
p-H2AX (S139)
PI (DNA content)

Figure S9

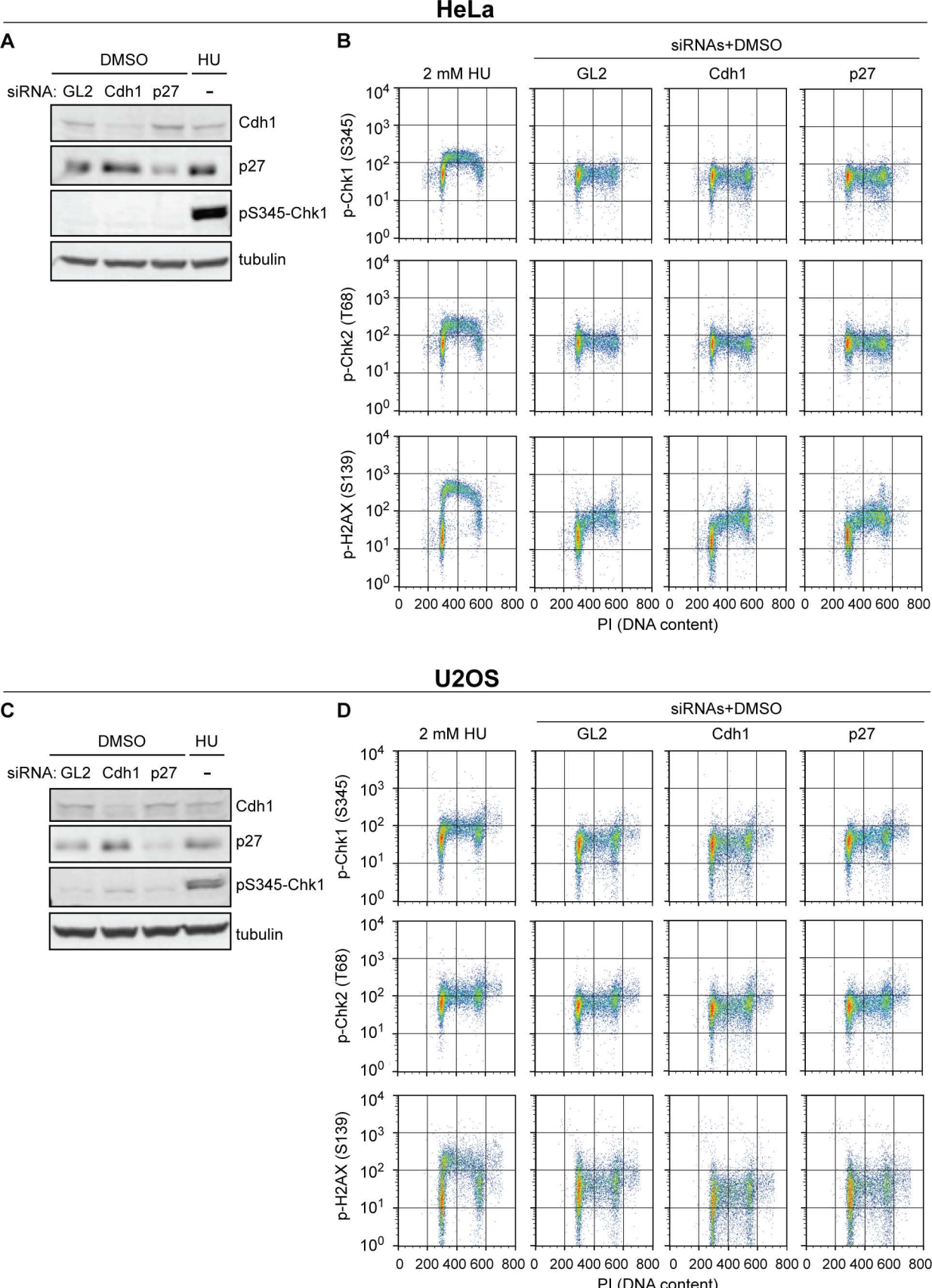
HeLa
A
DMSO
HU
siRNA: GL2 Cdh1 p27 -
Cdh1
p27
pS345-Chk1
tubulin
B
siRNAs+DMSO
2 mM HU
GL2
Cdh1
p27
p-Chk1 (S345)
p-Chk2 (T68)
p-H2AX (S139)
PI (DNA content)
U2OS
C
DMSO
HU
siRNA: GL2 Cdh1 p27 -
Cdh1
p27
pS345-Chk1
tubulin
D
siRNAs+DMSO
2 mM HU
GL2
Cdh1
p27
p-Chk1 (S345)
p-Chk2 (T68)
p-H2AX (S139)
PI (DNA content)

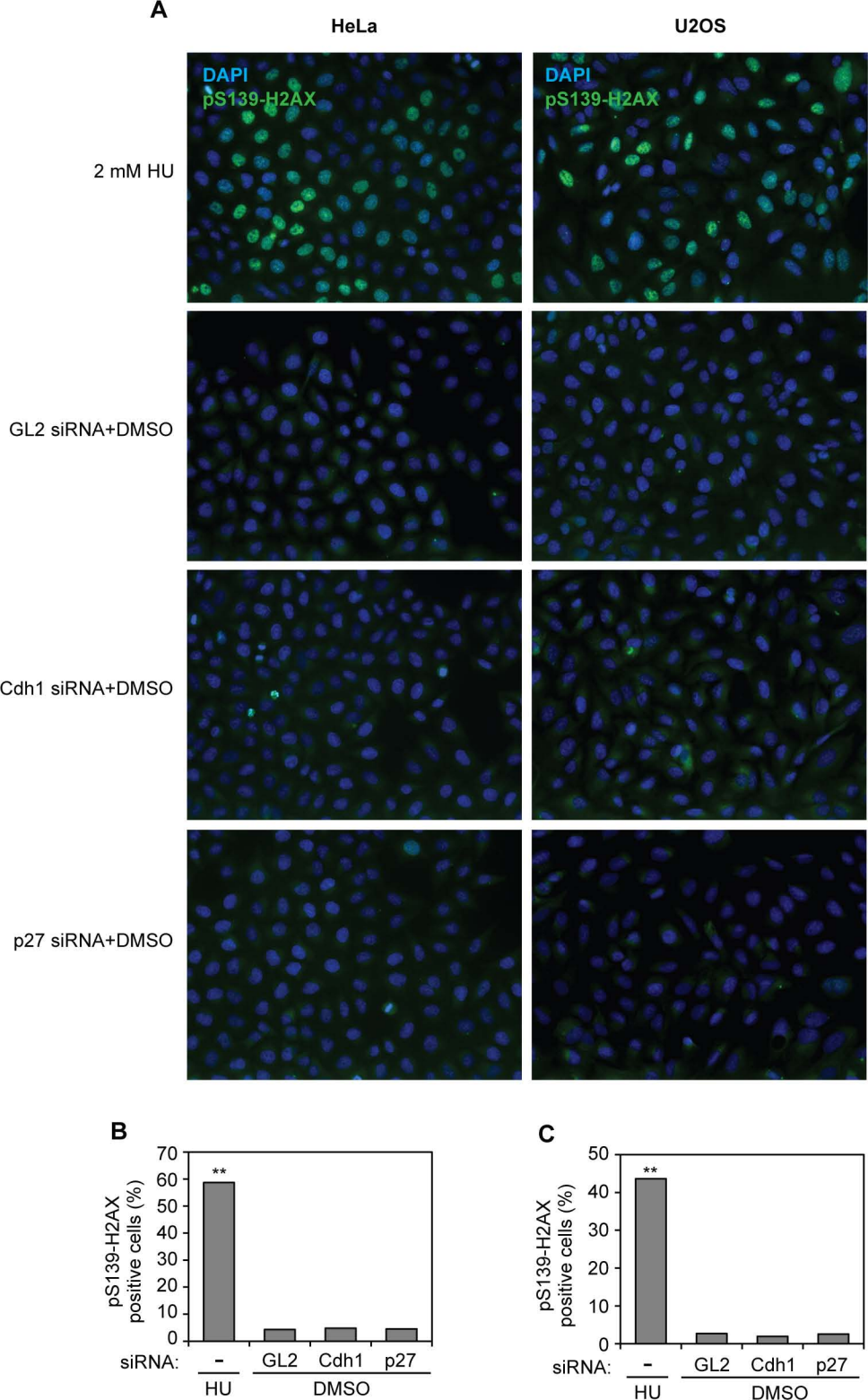
A
HeLa
U2OS
DAPI
pS139-H2AX
2 mM HU
GL2 siRNA+DMSO
Cdh1 siRNA+DMSO
p27 siRNA+DMSO
B
pS139-H2AX positive cells (%)
70
60
50
40
30
20
10
0
**
siRNA:
-
GL2
Cdh1
p27
HU
DMSO
C
pS139-H2AX positive cells (%)
50
40
30
20
10
0
**
siRNA:
-
GL2
Cdh1
p27
HU
DMSO